Pure and Applied Geophysics manuscript No.
(will be inserted by the editor)

Valuation of the optimal utility of some investment projects with environmental effects

I. Arregui · C. Vázquez

Received: date / Accepted: date

Abstract In this work the authors propose efficient numerical methods to solve mathematical models for different optimal investment problems with irreversible environmental effects. A relevant point is that both the benefits of the environment and the alternative project are uncertain. The cases with instantaneous and progressive transformation of the environment are addressed. In the first case, an Augmented Lagrangian Active Set (ALAS) algorithm combined with finite element methods are proposed as a more efficient technique for the numerical solution of the obstacle problem associated to a degenerated elliptic PDE. In the second case, the mathematical model can be split into two subsequent steps: first we solve numerically a set of parameter dependent boundary value problems (the parameter being the level of progressive transformation) and secondly an evolutive nonstandard obstacle problem is discretized, thus leading to an obstacle problem at each time step. Also ALAS algorithm is proposed at each time step. Numerical solutions are validated through qualitative properties theoretically proven in the literature for different examples.

Keywords Investment under uncertainty · obstacle problems · finite elements · augmented lagrangian algorithm

1 Introduction

Physiocrats economic school understood the Earth as the main source of health, so that Economics should focus on getting the most benefit from unlimited renewable Earth resources. Later, most economic schools separated the environment from the

This work is partially supported by MICINN (MTM2010-21135-C02-01) and by Xunta de Galicia (Ayuda CN2011/004 cofinanced with FEDER funds).

I. Arregui, C. Vázquez (Corresponding author)
Department of Mathematics, Faculty of Informatics, Campus Elviña s/n, 15071-A Coruña (Spain)
Tel.: +34-981167000
Fax: +34-981167160
E-mail: {arregui, carlosv}@udc.es

economic development, thus environmental resources being understood as an exogenous factor in the economy. More recently, the discipline of Environmental Economics incorporates classical tools from Economics to the analysis of environmental problems in order to focus economic activity to minimize negative effects on the Earth planet. Clearly, the tools of Applied Mathematics can be used for the modeling and solution of problems arising both in Economics and Environmental Sciences, and therefore in Environmental Economics. The present article can be framed in this general setting. More precisely, we focus on a problem arising in the economics of environmental management involving uncertain and irreversible effects.

Since the earlier civilizations, human action has changed planet Earth. Jointly with water, wind and vegetation, human action has become one of the main external agents acting on the environment. Traditionally, the effect of these agents are incorporated in the modeling of different geophysical phenomena [12]. In more recent times, the extremely quick advance of technology makes the human effect specially relevant. The building of new cities and the expansion of human habitat into previously unoccupied areas has also contributed to it, resulting in the construction of buildings, communications routes (roads, airports, railways, etc.) or infrastructures for the exploitation of natural resources (dams, ports, mines, terraces, etc.). Thus, in order to asses environmental policies, the impact of human actions in the different geophysical processes needs to be analyzed, mathematically modeled and numerically simulated.

In order to decide when and how best to invest in infrastructure or industrial projects it is important to consider not only the financial aspects but also the environmental impact of the investment. Also, an important aspect to consider is that their benefits will mainly occur in the future and future uncertain factors may be involved. The irreversibility of some actions on the environment represents also an important factor to be considered when starting investment projects.

In this work, we deal with the numerical solution of some models related to the opportunity of starting an industrial project that provides some uncertain benefits but also involves some irreversible effects on the environment. In the case of instantaneous irreversible effects, the implicit uncertain profit associated to the environment stops once the project is initiated. When both the environment and the industrial project benefits are uncertain and governed by stochastic processes, an important problem is to determine if the project should be started and which will be the joint utility if started at an optimal instant. In the case of a progressive transformation of the environment, the utility also depends on the evolution of the fraction of the environment that is being transformed. In [10] this kind of problems are studied and some analogies are established between them and those ones related to financial options pricing.

In [21], a first approach to the rigorous mathematical modeling of these kind of optimization problems is performed, its departure point being the one period example treated in [2] to discuss the so called *quasi-option* value. More precisely, in [21]

it is proved that the optimal utility function is the unique viscosity solution to the associated Hamilton–Jacobi–Bellman equation. Moreover, this optimal utility value function depends on the fraction of the environment that has been converted for the alternative project and from the initial profits associated to the environment and the alternative industrial project. More recently, in [8] a suitable change of variable allows to formulate the same problem in terms of two sequential PDE problems. The first one is associated to an elliptic degenerate PDE depending on a time parameter. The second can be formulated as an evolutive problem involving a multivalued operator. The model is mathematically analyzed by means of L^∞-accretive operators techniques. Although in [21] some analytical solutions are discussed for particular expressions of the utility function (additive HARA utility functions), numerical methods are clearly required for the general case. In the present paper, taking advantage of the equivalent formulation in [8], we propose some suitable numerical techniques to solve the general problem.

Moreover, in [9] the case of instantaneous irreversible effects on the environment is addressed. This case corresponds to a particular choice of the utility function. so that an obstacle problem associated to a second-order elliptic operator which is not in divergence form is posed. Under certain not too much restrictive hypotheses, by using the specific structure of the differential operator and the unbounded spatial domain, an appropriate change of variable is chosen in [9] to prove the existence and uniqueness of solution. Some regularity results and qualitative properties of the solution are also stated for specific choices of the data. As these properties cannot be stated for the general case, some numerical methods to compute approximated solutions have been proposed in [1]. More precisely, projected Gauss-Seidel [13] and Lions-Mercier [19] type algorithms for the discretized finite elements problem are applied. In the second case, the method is combined with a multigrid and adaptive refinement [14]. The numerical methods are validated by means of examples whose solutions exhibit proved qualitative properties in [9]. However, some of the techniques can be replaced for the more efficient ones we propose in the present paper.

In the present work, we propose different numerical techniques to solve the mathematical models analyzed in [8] and [9], proposed for the case of progressive and instantaneous effects on the environment, respectively. For this purpose, we consider a finite element discretization of the equivalent PDE problem posed on a suitable bounded domain, thus avoiding the required domain truncation of the original unbounded domain [15]. Moreover, in the case of instantaneous effects, we propose an augmented Lagrangian active set method as a more efficient alternative to those ones proposed in [1]. We also validate the qualitative properties of the solution of this problem in different particular cases. The same numerical techniques are adapted for the obstacle problems appearing in the PDE model for progressive transformation of the environment.

The outline of the paper is the following. In Section 2 we describe the mathematical models of the optimal investment problem in the case of progressive and instantaneous effects on the environment. In Section 3 we describe the proposed numerical

methods, mainly based on finite elements discretization and augmented Lagrangian active set method for the discretized obstacle problems. Section 4 is devoted to the numerical tests illustrating the good performance of the numerical methods and the qualitative properties of the numerical solutions. Finally, some conclusions are presented in Section 5.

2 Mathematical model

Let us consider a certain aspect related to the environment (a natural site, like a lake, a beach, a river or a mountain, for example) which can be developed into an alternative use (industrial plant, hotel, building, bridge, port, mine, tunnel, etc), the effects of which on the environment are irreversible. We assume that the benefits (per unit) of the original environment aspect and the alternative project are random. More precisely, we assume that the benefits (per unit) of the environmental aspect (by means of tourism, for example), at time $t \geq 0$ are given by the stochastic process X_t. Also, let us consider that the random benefits (per unit) associated to the alternative project (by means of transport facilities, mine resources, additional business companies, for example) are given by the stochastic process Y_t. The dynamics of both stochastic processes is governed by the following differential equations:

$$\begin{cases} dX_t = \mu_1(X_t)\,dt + \sqrt{2}\sigma_1(X_t)\,dB_{1_t}\,, & X_0 = x \in \mathbb{R} \\ dY_t = \mu_2(Y_t)\,dt + \sqrt{2}\sigma_2(Y_t)\,dB_{2_t}\,, & Y_0 = y \in \mathbb{R}\,, \end{cases} \tag{1}$$

where $\{B_{i_t}\}_{t\geq 0}$ are Brownian motions defined in a certain probability space, μ_1 and μ_2 represent the drift functions of processes X_t and Y_t, and σ_1 and σ_2 are the standard deviation functions. Although we can assume that for $i = 1, 2$ the functions μ_i and σ_i are Lipschitz continuous and vanishing at the origin as in [21,8], for simplicity we will consider them as constants, so that:

$$\mu_i(z) = \mu_i, \quad \sigma_i(z) = \sigma_i, \qquad i = 1, 2.$$

We also consider a constant correlation coefficient ρ so that $dX_t dY_t = \rho dt$. In more practical applications, these and other model parameters need to be calibrated from real data. For example, those ones concerning to environmental benefits could incorporate the output of some geophysical models related to the underlying particular environmental aspects that are involved.

As we consider a general case where only a part of the environment has been transformed into the industrial project, we denote by $\theta_t \in [0, 1]$ the transformed fraction of the environment at time t. We assume that

$$\theta_t = \theta + M_t \in [0, 1], \tag{2}$$

where M_t is a process describing the nonnegative and nondecreasing cumulative development starting with $M_0 = 0$. Notice that the initial data $X_0 = x$, $Y_0 = y$ and $\theta_0 = \theta \in [0, 1]$ are given.

In order to pose the optimization problem we need to consider a utility function U depending on two arguments. In the general case, we impose that U is concave and non-decreasing in their arguments and that $U(0,0) = 0$. As indicated in [21], cases where $U(0,0)$ is not finite require further developments in the theory (and also in numerics). As only a fraction of the environment is transformed into the alternative industrial project, the joint utility at time t is given by $U((1-\theta_t)X_t, \theta_t Y_t)$. In terms of this utility, the expected cumulative utility functional is defined by the expression

$$J(x,y,\theta) = \mathbb{E}\left[\int_0^{+\infty} e^{-\alpha s}\, U((1-\theta_s)X_s, \theta_s Y_s)\, ds\right], \tag{3}$$

where $\mathbb{E}$ represents the expected value, α denotes the constant continuous discount rate, X_t and Y_t follow equations (1) and θ_t satisfies condition (2). Moreover, let $\mathcal{A}_\theta$ denote the domain for M_t such that condition (2) holds.

Next, we pose the problem of determining the value function, v, associated to the utility functional (3) as

$$v(x,y,\theta) = \max_{\mathcal{A}_\theta} J(x,y,\theta))\,. \tag{4}$$

Notice that the utility function depends on the initial benefits of the environment (x) and the alternative project (y), which are assumed to be nonnegative, and also on the initial fraction of the environment (θ) that is transformed.

Additionally, in [21] for the case of constant μ_i and σ_i the authors focus on additive HARA utility functions in the form:

$$U(x,y) = \frac{(x+y)^p}{p}, \tag{5}$$

where $1-p$ represents the constant relative risk aversion parameter (so that $p = 1$ corresponds to risk-neutrality). In this case, U has homogeneity of degree p and the linearity of the state equations for X_t and Y_t implies the homogeneity of the value function and a possibility to reduce the dimension of the equation. Notice that the limit case $p \to 0$ corresponds to logarithmic utility that fails out of the hypothesis $U(0,0) = 0$ (or even $U(0,0)$ finite), thus requiring further research. In the numerical results sections we mainly address examples with the utility function defined by (5).

In the next section, we recall the PDE models corresponding to two situations: first, when a fraction of the environment is progressively transformed [8] and, secondly, when the environment is instantaneously transformed [9] into the alternative industrial problem.

2.1 PDE model with progressive transformation of the environment

By using the theory of viscosity solutions [7] or the arguments in [8], the following Hamilton-Jacobi-Bellman (HJB) equation can be obtained:

$$\min[-\mathcal{L}v + \alpha v - U((1-\theta)x, \theta y), -v_\theta] = 0, \quad \text{in } \Omega, \tag{6}$$

where $\Omega = (0,+\infty)\times(0,+\infty)$ and $\mathcal{L}$ is the second order differential operator defined by:

$$\mathcal{L}v = \sigma_1^2 x^2 v_{xx} + \sigma_2^2 y^2 v_{yy} + 2\sigma_1\sigma_2\rho xy v_{xy} + \mu_1 x v_x + \mu_2 y v_y\,. \tag{7}$$

Actually, by introducing the matrix A and the vector $\mathbf{b}$ given by:

$$A(x,y) = \begin{pmatrix} \sigma_1^2 x^2 & \sigma_1\sigma_2\rho xy \\ \sigma_1\sigma_2\rho xy & \sigma_2^2 y^2 \end{pmatrix}, \qquad \mathbf{b}(x,y) = \begin{pmatrix} (\mu_1 - 2\sigma_1^2 - \sigma_1\sigma_2\rho)x \\ (\mu_2 - 2\sigma_2^2 - \sigma_1\sigma_2\rho)y \end{pmatrix},$$

we can write (7) in the following divergence form:

$$\mathcal{L}v = \operatorname{div}(A\,\nabla v) + \mathbf{b}\cdot\nabla v\,.$$

Notice that at the boundaries $x = 0$ and $y = 0$, the operator (7) degenerates and homogeneous Neumann-like boundary conditions are implicit. Moreover, we introduce the function

$$\hat{U}(x,y,\theta) = U((1-\theta)x, \theta y)$$

and notice that when we reach $\theta = 1$ all the environment has been transformed into the alternative problem so that we have:

$$v(x,y,1) = \mathbb{E}\left[\int_0^{+\infty} e^{-\alpha s}\, U((0,Y(s))\,ds\right].$$

So, the HJB equation (6) jointly with homogeneous Neumann boundary condition and the value with $\theta = 1$ can be written in the form:

$$\begin{cases} \min[-\mathcal{L}v + \alpha v - \hat{U}, -v_\theta] = 0, & \text{in } \Omega\times(0,1), \\ A\nabla v\cdot\boldsymbol{\nu} = 0, & \text{in } \partial\Omega\times(0,1), \\ v(x,y,1) = \mathbb{E}\left[\displaystyle\int_0^{+\infty} e^{-\alpha s}\, U(0,Y(s))\,ds\right], & \text{in } \Omega, \end{cases} \tag{8}$$

where $\boldsymbol{\nu}$ denotes the unit normal vector to $\partial\Omega$.

Moreover, in [8] the change of variable $t = 1-\theta$ and the function

$$\overline{U}(x,y,t) = \hat{U}(x,y,1-t) = U(tx,(1-t)y)$$

are introduced, so that the following auxiliary problem is considered:

$$\begin{cases} -\mathcal{L}f + \alpha f = \overline{U}(\cdot,\cdot,t), & \text{in } \Omega\times(0,1), \\ A\nabla f\cdot\boldsymbol{\nu} = 0, & \text{in } \partial\Omega\times(0,1). \end{cases} \tag{9}$$

By using the solution of (9) to introduce the new unknown

$$u(x,y,t) = v(x,y,1-t) - f(x,y,t), \tag{10}$$

then problem (8) can be written as the following evolutive problem

$$\begin{cases} \min[u_t + f_t, -\mathcal{L}v + \alpha v - \hat{U}] = 0, & \text{in } \Omega\times(0,1), \\ A\nabla u\cdot\boldsymbol{\nu} = 0, & \text{in } \partial\Omega\times(0,1), \\ u(x,y,0) = \mathbb{E}\left[\displaystyle\int_0^{+\infty} e^{-\alpha s}\, U(0,Y(s))\,ds\right] - f(x,y,0), & \text{in } \Omega. \end{cases} \tag{11}$$

In [8] a suitable multivalued operator is introduced to pose an equivalent formulation to (11) with an homogeneous initial condition so that existence of solutions is obtained by using L^∞ accretive operators theory.

In the section of numerical methods we propose a strategy to solve problem (6) by sequentially solving problems (9) and (11).

2.2 PDE model with instantaneous transformation of the environment

In this section we assume instantaneous irreversible effects on the environment. If the project is developed at time T then the expected cumulative utility functional is given by

$$\begin{aligned} J(x,y;T) &= \mathbb{E}\left[\int_0^T e^{-\alpha s}X(s)\,ds + \int_T^{+\infty} e^{-\alpha s}Y(s)\,ds\right] = \\ &= \mathbb{E}\left[\int_0^{+\infty} \left(\mathbb{I}_{[0,T]}e^{-\alpha s}X(s) + \mathbb{I}_{[T,+\infty)}e^{-\alpha s}Y(s)\right)\,ds\right], \end{aligned}$$

where $\mathbb{I}_C$ represents the characteristic function of set C. In order to model more general problems, we can consider the following utility function:

$$J(x,y;T) = \mathbb{E}\left[\int_0^{+\infty} e^{-\alpha s}\,\left(\mathbb{I}_{[0,T]}f(X(s)) + \mathbb{I}_{[T,+\infty]}Y(s)\right)\,ds\right] \tag{12}$$

for a given function f.

Thus, analogously to the general case we pose the problem of determining the value, v, which is obtained when the alternative project is started at the optimal instant, T, that is:

$$v(x,y) = \max_T J(x,y;T)\,.$$

Notice that the value function depends on the initial benefits of the environment (x) and the alternative project (y), which are assumed to be nonnegative.

Next, using Bensoussan–Lions [3] techniques, it is easy to prove that function v is the solution of the following linear complementarity problem, posed on the domain $\Omega = (0,+\infty)\times(0,+\infty)$:

$$-\mathcal{L}v + \alpha v \geq f, \qquad v \geq h, \qquad (-\mathcal{L}v + \alpha v - f)(v-h) = 0, \tag{13}$$

where $\mathcal{L}$ is given by (7) and the lower obstacle, h, is the obtained utility when the project is started at time $T = 0$ (i.e., $h(x,y) = J(x,y,0)$). Thus, the analytical expression of function h is given by:

$$h(x,y) = \mathbb{E}\left[\int_0^{+\infty} e^{-\alpha s}Y(s)\,ds\right] = \frac{y}{(\lambda-1)(\sigma_2^2\lambda + \mu_2)}\,, \tag{14}$$

with

$$\lambda = \frac{1}{2}\left[\left(1-\frac{\mu_2}{\sigma_2}\right) - \sqrt{\left(1-\frac{\mu_2}{\sigma_2}\right)+\frac{4\alpha}{\sigma_2^2}}\right] . \tag{15}$$

On the other hand, if we introduce a new unknown $u = v - h$, the equivalent problem to obtain u can be written as:

$$-\mathcal{L}u + \alpha u \geq G, \qquad u \geq 0, \qquad (-\mathcal{L}u + \alpha u - G)u = 0\,, \tag{16}$$

which is still posed on the unbounded domain Ω. Notice that $G = f + \mathcal{L}h - \alpha h$ and the associated obstacle function is identically zero. Moreover, due to the expression of matrix A, the homogeneous Neumann boundary condition $(A\nabla u)\cdot\boldsymbol{\nu} = 0$ is again naturally obtained on the boundaries $x = 0$ and $y = 0$.

In order to overcome the difficulty due to the unboundness of Ω, we use the following change of variable proposed in [9]:

$$\theta = \arctan x \qquad\qquad \beta = \arctan y\,, \tag{17}$$

that maps the domain Ω into $\mathcal{F}(\Omega) = (0,\pi/2)\times(0,\pi/2)$, where $\mathcal{F}(x,y) = (\theta(x,y),\beta(x,y))$. Thus, the equivalent complementarity problem consists on finding $\widehat{u}$, defined by $\widehat{u} = u\circ\mathcal{F}^{-1}$, such that:

$$-\mathcal{L}_{(\theta,\beta)}\widehat{u} + \alpha\widehat{u} \geq \widehat{G}, \qquad \widehat{u} \geq 0, \qquad (-\mathcal{L}_{(\theta,\beta)}\widehat{u} + \alpha\widehat{u} - \widehat{G})\widehat{u} = 0\,, \tag{18}$$

where:

$$\mathcal{L}_{(\theta,\beta)}\widehat{u} = \text{div}_{\,(\theta,\beta)}(S\nabla_{(\theta,\beta)}\widehat{u}) + \mathbf{p}\cdot\nabla_{(\theta,\beta)}\widehat{u}\,, \qquad\qquad \widehat{G} = G\circ\mathcal{F}^{-1}\,,$$

and the subindex in the differential operators refers to the involved spatial variables. Moreover, matrix S and vector $\mathbf{p}$ are given by:

$$S = \begin{pmatrix} \frac{\sigma_1^2}{4}\sin^2 2\theta & \frac{\sigma_1\sigma_2\rho}{4}\sin 2\theta\sin 2\beta \\ \\ \frac{\sigma_1\sigma_2\rho}{4}\sin 2\theta\sin 2\beta & \frac{\sigma_2^2}{4}\sin^2 2\beta \end{pmatrix},$$

$$\mathbf{p} = \begin{pmatrix} \dfrac{\sin 2\theta}{2}(\mu_1 - 2\sigma_1^2\cos^2\theta - \sigma_1\sigma_2\rho\cos 2\beta) \\ \\ \dfrac{\sin 2\beta}{2}(\mu_2 - 2\sigma_2^2\cos^2\beta - \sigma_1\sigma_2\rho\cos 2\theta) \end{pmatrix}.$$

Following [9], we assume that there exist some parameters $m_1 > 1$ and $m_2 > 1$ such that:

$$\omega^{1/2}G = (1+x^2)^{-m_1/2}(1+y^2)^{-m_2/2}G \in L^2(\Omega)\,, \tag{19}$$

which is equivalent to assume that $\widehat{\omega}^{1/2}\widehat{G} \in L^2(\mathcal{F}(\Omega))$, with $\widehat{\omega} = \omega\circ\mathcal{F}^{-1}$.

Next, we consider the weighted Sobolev spaces:

$$L^2_\omega(\mathcal{F}(\Omega)) = \left\{\varphi \,:\, \widehat{\omega}^{1/2}\varphi \in L^2(\mathcal{F}(\Omega))\right\}$$
$$H^1_\omega(\mathcal{F}(\Omega), S) = \left\{\varphi \in L^2_\omega(\mathcal{F}(\Omega)) \,:\, (\sin 2\theta)\varphi_\theta \in L^2_\omega(\mathcal{F}(\Omega)),\ (\sin 2\beta)\varphi_\beta \in L^2_\omega(\mathcal{F}(\Omega))\right\}$$

and the convex set:

$$\widehat{\mathcal{K}} = \left\{\varphi \in H^1_\omega(\mathcal{F}(\Omega), S) \,:\, \varphi \geq 0\right\} .$$

Thus, the problem (18) admits the following variational inequality formulation:

Find $u \in \widehat{\mathcal{K}}$, such that:

$$a(\widehat{u}, \varphi - \widehat{u}) \geq L(\varphi - \widehat{u}) , \quad \forall \varphi \in \widehat{\mathcal{K}}, \tag{20}$$

where the bilinear form a and linear operator L are given by:

$$a(\widehat{u}, \varphi) = \int_{\mathcal{F}(\Omega)} \widehat{\omega} \left\{\nabla\varphi \cdot S\nabla\widehat{u} + \left[\left(\frac{1}{\widehat{\omega}}\nabla\widehat{\omega} \cdot S - \mathbf{p}\cdot\right)\nabla\widehat{u}\right]\varphi + \alpha\widehat{u}\varphi\right\} d\theta\, d\beta$$
$$L(\varphi) = \int_{\mathcal{F}(\Omega)} (\widehat{\omega}\,\widehat{G}\,\varphi)\, d\theta\, d\beta .$$

The existence and uniqueness of solution for (20) are proven in [9] for the case $\mu_1 = \mu_2 = 0$ and in [11] without this assumption.

By using formulation (20), in [1] a set of numerical techniques to solve this problem have been proposed. In next section, we propose new ones which improve the efficiency in the numerical solution and can also be used for the model with progressive transformation of the environment.

3 Numerical methods

3.1 Numerical solution of the model for instantaneous transformation

First, in order to discretize the continuous problem (20), let us consider a family of finite element triangular meshes (τ_h) of $\mathcal{F}(\Omega)$ for $h > 0$. Each mesh is formed by elements of diameter less than or equal to h and we denote its set of nodes by

$$\Sigma_h = \bigcup_{T\in\tau_h} \Sigma_T = \bigcup_{T\in\tau_h} \{a_i \mid 1 \leq i \leq N\} ,$$

where Σ_T denotes the set of nodes in the mesh triangle T. Next, we define the space of piecewise linear Lagrange finite elements:

$$V_h = \left\{\varphi_h \in \mathcal{C}^0(\overline{\Omega}) \,:\, \varphi_h|_T \in P_1 , \quad \forall T \in \tau_h\right\},$$

where P_1 denotes the space of polinomials of degree less or equal than one, and the convex set:

$$K_h = \{\varphi_h \in V_h \,:\, v_h(a_i) \geq 0, \forall a_i \in \Sigma_h\} . \tag{21}$$

Next, we pose the following discretized variational inequality problem:

Find $\widehat{u}_h \in K_h$ such that:

$$a(\widehat{u}_h, \varphi_h - \widehat{u}_h) \geq L(\varphi_h - \widehat{u}_h)\,, \qquad \forall \varphi_h \in K_h\,. \tag{22}$$

In order to introduce a matrix formulation of problem (22), we can choose the finite element space basis:

$$B = \{\psi_i \in V_h\,, \quad \psi_i(a_j) = \delta_{ij}\,, \quad 1 \leq i, j \leq N\}\,.$$

So, every function $\varphi_h \in V_h$ can be uniquely expressed in terms of the basis elements as:

$$\varphi_h = \sum_{i=1}^{N} \varphi_h(a_i)\psi_i\,.$$

Moreover, we introduce the vector of node values, $\bar{\varphi}_h$, defined by $(\bar{\varphi}_h)_i = \varphi_h(a_i)$, $1 \leq i \leq N$ and the finite element discretization matrix and vector

$$A_{ij} = a(\psi_j, \psi_i), \qquad b_i = L(\psi_i), \qquad 1 \leq i, j \leq N.$$

Thus, problem (22) can be written in the form

$$A_h \bar{u}_h \geq b_h, \qquad \bar{u}_h \geq 0, \qquad (A_h \bar{u}_h - b_h)\bar{u}_h = 0\,, \tag{23}$$

with the vector and matrix notations $A_h = (A_{ij})$ and $b_h = (b_i)$, respectively.

Different classical techniques exist for the numerical solution of discretized elliptic variational inequalities with unilateral constraints (see [13], for example). Among them, projected relaxation methods applied to the discretized problem can be chosen, having in mind that the convergence of these methods highly depends on the value of the relaxation parameter. In [1], we analyzed a comparison between projected Gauss-Seidel and Lions-Mercier [19], this last one combined with a multigrid technique and adaptive refinement. In the present paper, to solve problem (23) we propose the use of the more recent augmented Lagrangian active set (ALAS) algorithm [16]. The method has been previously used for several models from quantitative finance (see [4] or [6], for example).

More precisely, after the finite element discretization the discrete problem can be written in the form:

$$A_h \bar{u}_h + P_h = b_h, \tag{24}$$

with the discrete complementarity conditions

$$\bar{u}_h \geq 0, \quad P_h \leq 0, \quad \bar{u}_h P_h = 0, \tag{25}$$

where P_h denotes the vector of the multiplier values associated to the inequality constraint.

The basic iteration of the ALAS algorithm consists of two steps. In the first one the domain is decomposed into active and inactive parts (depending on whether the

constraints are active or not), and in the second step, a reduced linear system associated to the inactive part is solved. Thus, we use the algorithm for unilateral problems, which are based on the augmented Lagrangian formulation.

First, for any decomposition $\mathcal{N} = \mathcal{I} \cup \mathcal{J}$, where $\mathcal{N} := \{1, 2, \dots N_{\text{dof}}\}$, let us denote by $[A_h]_{\mathcal{I}\mathcal{I}}$ the principal minor of matrix A_h and by $[A_h]_{\mathcal{I}\mathcal{J}}$ the co-diagonal block indexed by $\mathcal{I}$ and $\mathcal{J}$. Thus, the ALAS algorithm computes not only $\bar{u}_h$ and P_h but also a decomposition $\mathcal{N} = \mathcal{J} \cup \mathcal{I}$ such that

$$\begin{aligned} A_h \bar{u}_h + P_h &= b_h, \\ [P_h]_j + \beta\, [\bar{u}_h]_j &\le 0, \qquad && \forall j \in \mathcal{J}, \\ [P_h]_i &= 0, && \forall i \in \mathcal{I}, \end{aligned} \tag{26}$$

for a given positive parameter β. In the above equations, $\mathcal{I}$ and $\mathcal{J}$ are the *inactive* and the *active* sets, respectively. More precisely, the iterative algorithm builds sequences $\{\bar{u}_h^m\}_m$, $\{P_h^m\}_m$, $\{\mathcal{I}^m\}_m$ and $\{\mathcal{J}^m\}_m$, converging to $\bar{u}_h$, P_h, $\mathcal{I}$ and $\mathcal{J}$, by means of the following steps:

1. Initialize $\bar{u}_h^0 = 0$ and $P_h^0 = \min\{b_h - A_h \bar{u}_h^0, 0\} \le 0$. Choose $\beta > 0$. Set $m = 0$.
2. Compute

$$\begin{aligned} Q_h^m &= \min\left\{0, P_h^m + \beta\,(\bar{u}_h^m - 0)\right\}, \\ \mathcal{J}^m &= \left\{ j \in \mathcal{N}, [Q_h^m]_j < 0 \right\}, \\ \mathcal{I}^m &= \{ i \in \mathcal{N}, [Q_h^m]_i = 0 \}. \end{aligned}$$

3. If $m \ge 1$ and $\mathcal{J}^m = \mathcal{J}^{m-1}$ then convergence is achieved. Stop.
4. Let $\bar{u}$ and P be the solution of the linear system:

$$\begin{aligned} &A_h \bar{u} + P = b_h, \\ &P = 0 \quad \text{on} \quad \mathcal{I}^m \quad \text{and} \quad \bar{u} = 0 \quad \text{on} \quad \mathcal{J}^m. \end{aligned} \tag{27}$$

Set $\bar{u}_h^{m+1} = V$, $P_h^{m+1} = \min\{0, P\}$, $m = m + 1$ and go to Step 2.

It is important to notice that, instead of solving the full linear system in (27), for $\mathcal{I} = \mathcal{I}^m$ and $\mathcal{J} = \mathcal{J}^m$ the following reduced one on the inactive set is solved:

$$\begin{aligned} [A_h]_{\mathcal{I}\mathcal{I}}\, [\bar{u}]_{\mathcal{I}} &= [b_h]_{\mathcal{I}}\,, \\ [\bar{u}]_{\mathcal{J}} &= 0_J, \\ P &= b - A_h \bar{u}. \end{aligned} \tag{28}$$

In [16], the convergence of the algorithm in a finite number of steps is proved for a Stieltjes matrix (i.e. a real symmetric positive definite matrix with negative off-diagonal entries) and a suitable initialization (the same we consider in this paper). They also prove that $\mathcal{I}^m \subset \mathcal{I}^{m+1}$. A Stieltjes matrix is obtained for linear elements.

Also we have implemented a refinement criterium that selects the elements where

$$u_h(a_i) > 0 \quad \text{and} \quad u_h(a_j) = 0\,, \quad \text{for } i \ne j \text{ in } \{1, 2, 3\}\,,$$

a_i being the vertices of the triangle. So, elements close to the free boundary are refined. Once one element has been selected for refinement, we implement the refinement technique proposed in [20].

In Section 4.1. some examples illustrate the performance of the described numerical strategy for the case of instantaneous transformation of the environment. Also the method is compared with projected Gauss-Seidel, specially in terms of computational time.

3.2 Numerical solution of the model for progressive transformation

In order to numerically solve problem (11), we start writing the first equation in (11) in the following equivalent form:

$$u_t + f_t \geq 0, \quad -\mathcal{L}u + \alpha u \geq 0, \quad (u_t + f_t)\,(-\mathcal{L}u + \alpha u) = 0. \qquad \text{in } \Omega \times (0,1) \tag{29}$$

In order to discretize in variable t the previous equation, we consider a natural number $N > 0$, the stepsize $\Delta t = 1/(N+1)$ and the discrete values $t^n = n\Delta t$, for $t = 0, 1, \ldots, N+1$. Moreover, we introduce the functional notation $h^n = h(\cdot, t = t^n))$ for all functions depending on $(x, y) \in \Omega$ and $t \in [0, 1]$ and propose the following approximation:

$$(u_t + f_t)(\cdot, t^n) = \frac{u^n - u^{n-1}}{\Delta t} + \frac{f^n - f^{n-1}}{\Delta t}. \tag{30}$$

Thus, by introducing approximation (30) in equations (29), after initializing $u^0 = u(\cdot, 0)$ we sequentially compute u^n as the solution of the complementarity problem

$$u^n \geq \psi^n, \ -\mathcal{L}u^n + \alpha u^n \geq 0, \ (u^n - \psi^n)\,(-\mathcal{L}u^n + \alpha u^n) = 0, \qquad \text{in } \Omega, \tag{31}$$

jointly with homogeneous Neumann boundary conditions, where

$$\psi^n = u^{n-1} - f^n + f^{n-1} \tag{32}$$

represents the obstacle function at each step of variable t.

Notice that for each step n, problem (31) is analogous to problem (16) appearing in the instantaneous transformation case, although with a nonzero obstacle function ψ^n and a null second member of the equation instead of G.

The terms f^n are previously computed by solving problem (9) for the different values $t = t^n$. For the numerical solution of problem (9) we use the same finite element discretization as in the instantaneous transformation case, so that the discretized problem takes the form:

$$A_h \bar{f}_h^n = b_h^n,$$

where b_h^n denotes the second member associated to the function $\overline{U}(\cdot, t^n)$ appearing in (9). The linear systems are solved by means of a classical LU factorization direct method.

For the numerical solution of (31), after the change of variable (17) to work in a bounded computational domain, we also propose the same finite elements discretization as in the other problems. Thus, the mixed formulation of the discretized problem can be written in the form:

$$A_h \bar{u}_h^n + P_h^n = 0, \tag{33}$$

with the discrete complementarity conditions

$$\bar{u}_h^n \geq \overline{\psi}_h^n, \quad P_h^n \leq 0, \quad \left(\bar{u}_h^n - \overline{\psi}_h^n\right) P_h^n = 0, \tag{34}$$

where P_h^n denotes the vector of the multiplier values and $\overline{\psi}_h^n$ denotes the vector of the nodal values defined by function ψ^n.

We apply the ALAS algorithm for solving formulation (34). More precisely, for each value t^n, the ALAS algorithm computes not only $\bar{u}_h^n$ and P_h^n but also a decomposition $\mathcal{N} = \mathcal{J}^n \cup \mathcal{I}^n$ such that

$$\begin{aligned} A_h \bar{u}_h^n + P_h^n &= 0, \\ [P_h^n]_j + \beta \left[\bar{u}_h^n - \overline{\psi}\right]_j &\leq 0, \qquad \forall j \in \mathcal{J}^n, \\ [P_h^n]_i &= 0, \qquad \forall i \in \mathcal{I}^n, \end{aligned} \tag{35}$$

for a given positive parameter β. In the above equations, $\mathcal{I}^n$ and $\mathcal{J}^n$ are the *inactive* and the *active* sets at t_n, respectively. More precisely, the iterative algorithm builds sequences $\left\{\bar{u}_{h,m}^n\right\}_m$, $\left\{P_{h,m}^n\right\}_m$, $\{\mathcal{I}_m^n\}_m$ and $\{\mathcal{J}_m^n\}_m$, converging to $\bar{u}_h^n$, P_h^n, $\mathcal{I}^n$ and $\mathcal{J}^n$, by means of the following steps:

1. Initialize $\bar{u}_{h,0}^n = \overline{\psi}_h^n$ and $P_{h,0}^n = \min\{b_h^n - A_h V_{h,0}^n, 0\} \leq 0$. Choose $\beta > 0$. Set $m = 0$.
2. Compute
$$\begin{aligned} Q_{h,m}^n &= \min\left\{0, P_{h,m}^n + \beta\left(\bar{u}_{h,m}^n - \overline{\psi}_{h,m}^n\right)\right\}, \\ \mathcal{J}_m^n &= \left\{j \in \mathcal{N}, \left[Q_{h,m}^n\right]_j < 0\right\}, \\ \mathcal{I}_m^n &= \{i \in \mathcal{N}, \left[Q_{h,m}^n\right]_i = 0\}. \end{aligned}$$
3. If $m \geq 1$ and $\mathcal{J}_m^n = \mathcal{J}_{m-1}^n$ then convergence is achieved. Stop.
4. Let $\bar{u}$ and P be the solution of the linear system
$$\begin{aligned} &A_h \bar{u} + P = 0, \\ &P = 0 \quad \text{on} \quad \mathcal{I}_m^n \quad \text{and} \quad \bar{u} = \overline{\psi}_{h,m}^n \quad \text{on} \quad \mathcal{J}_m^n. \end{aligned} \tag{36}$$
Set $\bar{u}_{h,m+1}^n = \bar{u}$, $P_{h,m+1}^n = \min\{0, P\}$, $m = m + 1$ and go to Step 2.

As in the instantaneous transformation case, instead of solving the full linear system in (36), for $\mathcal{I} = \mathcal{I}_m^n$ and $\mathcal{J} = \mathcal{J}_m^n$ the following reduced one on the inactive set is solved:

$$\begin{aligned} [A_h]_{\mathcal{I}\mathcal{I}} [\bar{u}]_{\mathcal{I}} &= -[A_h]_{\mathcal{I}\mathcal{J}} \left[\overline{\psi}\right]_{\mathcal{J}}, \\ [\bar{u}]_{\mathcal{J}} &= \left[\overline{\psi}\right]_{\mathcal{J}}, \\ P &= -A_h \bar{u}. \end{aligned} \tag{37}$$

4 Numerical results

4.1 Examples with instantaneous transformation

As in [1], in the present paper we first validate the proposed numerical methods by solving one example with known analytical solution. Next, we consider an example for which theoretically stated qualitative properties have been proved in [9] and [11]. The third example corresponds to a more realistic function h given by (14) in terms of the financial data.

Example 1:

In this example we choose $f(x) = x$ and $h(x, y) = c/\alpha$, c being a constant, so that $G(x, y) = x - c$. So, we assume a linear behaviour of the utility associated to environment with respect to the benefit (per unit) of the environment and that the utility of the alternative project is constant. Table 1 shows the set of model parameters. With these parameters, the exact solution (which only depends on x) is given by:

$$v(x,y) = \begin{cases} \dfrac{c^{1-\gamma}}{\alpha(1-\gamma)^{1-\gamma}|\gamma|^{\gamma}} x^{\gamma} + \dfrac{x}{\alpha} & \text{if } x \geq x_f \\ \dfrac{c}{\alpha} & \text{if } x \leq x_f, \end{cases}$$

with

$$\gamma = \frac{1}{2}\left(1 - \sqrt{1 + \frac{4\alpha}{\sigma_1^2}}\right), \qquad x_f = \frac{\gamma}{\gamma - 1} c\,.$$

Notice that the free boundary that separates the region where $v > h$ from the one with $v = h$ is the straight line $x = x_f$.

σ_1	σ_2	μ_1	μ_2	ρ	α	c
0.18	0.0	0.0	0.0	0.0	1.0	1.0

Table 1 Financial data set for Example 1

Table 2 summarizes the numerical results for up to five refinement levels starting from a uniform initial mesh with 289 nodes and 512 triangular elements. For both projected Gauss–Seidel and ALAS algorithms the stopping test in the relative quadratic error between two iterations is set to 10^{-5}, while for ALAS the parameter $\beta = 10000$ is chosen. In Table 2 we can observe that the relative error (e) with respect to the analytical solution is very close in both algorithms, the ALAS algorithm reports much shorter computational time (t) and less iterations (I).

Figure 1 shows the meshes of the domain $\mathcal{F}(\Omega)$ after five refinement levels ($L = 5$). Notice that the one corresponding to ALAS seems to better follow the

	ALAS					Projected Gauss–Seidel				
L	NE	NN	t_A	I_A	e_A	NE	NN	t_{GS}	I_{GS}	e_{GS}
1	512	289	4.39	2	6.92×10^{-3}	512	289	45.20	56	6.41×10^{-3}
2	704	386	7.10	4	6.03×10^{-3}	714	391	90.55	62	5.68×10^{-3}
3	1136	605	14.94	6	6.07×10^{-3}	1130	601	234.66	69	4.91×10^{-3}
4	2096	1087	40.51	7	4.80×10^{-3}	2153	1115	1819.61	160	4.58×10^{-3}
5	3840	1982	100.86	10	3.61×10^{-3}	4070	2076	8064.63	218	3.79×10^{-3}

Table 2 Mesh refinement, computational time, iterations and errors obtained for Example 1. L, NE, NN, t, I and e represent the level of refinement, number of elements, number of nodes, computational time in seconds, number of iterations and relative error, respectively. When appearing, subindex A refers to ALAS algorithm and GS to projected Gauss-Seidel

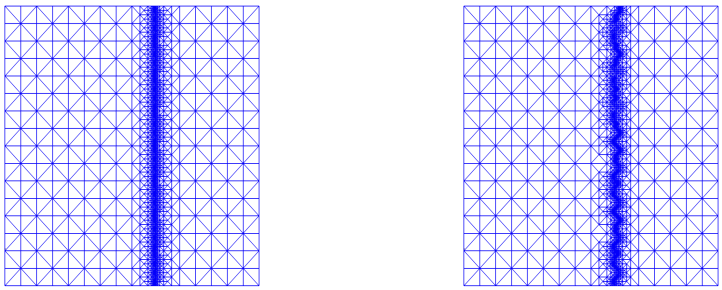

Fig. 1 Adaptive meshes of the domain $\mathcal{F}(\Omega)$ for ALAS (left) and projected Gauss-Seidel (right), after 5 refinement steps for Example 1

free-boundary of the problem. However, the error in both approximations is of the same order.

Example 2:

We choose $f(x) = x$ and $h(x, y) = y/\alpha$ so that $G(x, y) = x - y$ and utilities associated to environment and alternative project linearly depend on their respective benefits (per unit). The chosen parameters are shown in Table 3. Notice that in this example both volatilities and the correlation coefficient are different from zero.

σ_1	σ_2	μ_1	μ_2	ρ	α	c
0.18	0.40	0.0	0.0	0.20	1.0	1.0

Table 3 Financial data set for Example 2

Although we cannot obtain the expression of the exact solution, for the case $\mu_1 = \mu_2 = 0$ and $c > 0$ the following upper bound for the solution is stated in [9]:

$$\bar{u}(x,y) = \begin{cases} \dfrac{y}{\alpha}\,, & \text{if } (x,y) \in \Omega_1 \\ \dfrac{(\delta-1)^{\delta-1}}{\alpha c^{\delta-1}\delta^{\delta}} y^{\delta} + \dfrac{c}{\alpha}\,, & \text{if } (x,y) \in \Omega_2 \\ \dfrac{c^{1-\gamma}}{\alpha(1-\gamma)^{1-\gamma} \mid \gamma \mid^{\gamma}} x^{\gamma} + \dfrac{x}{\alpha} + \dfrac{(\delta-1)^{\delta-1}}{\alpha c^{\delta-1}\delta^{\delta}} y^{\delta}\,, & \text{if } (x,y) \in \Omega_3 \\ \dfrac{c^{1-\gamma}}{\alpha(1-\gamma)^{1-\gamma} \mid \gamma \mid^{\gamma}} x^{\gamma} + \dfrac{x}{\alpha} + \dfrac{y-c}{\alpha}\,, & \text{if } (x,y) \in \Omega_4 \end{cases}$$

where

$$\begin{aligned} \Omega_1 &= \left\{ (x,y) \in \Omega \,:\, x \le \frac{\gamma}{\gamma-1} c \quad \text{and} \quad y \ge \frac{\delta}{\delta-1} c \right\} \\ \Omega_2 &= \left\{ (x,y) \in \Omega \,:\, x \le \frac{\gamma}{\gamma-1} c \quad \text{and} \quad y \le \frac{\delta}{\delta-1} c \right\} \\ \Omega_3 &= \left\{ (x,y) \in \Omega \,:\, x \ge \frac{\gamma}{\gamma-1} c \quad \text{and} \quad y \le \frac{\delta}{\delta-1} c \right\} \\ \Omega_4 &= \left\{ (x,y) \in \Omega \,:\, x \ge \frac{\gamma}{\gamma-1} c \quad \text{and} \quad y \ge \frac{\delta}{\delta-1} c \right\}. \end{aligned}$$

Morover, as stated in [11], we can identify the following subset, S_C, of the coincidence set characterized by the condition:

$$S_C \;=\; \{(x,y) \in \Omega\,,\, y \ge \gamma x\} \subset \{(x,y) \in \Omega\,,\, u(x,y) = h(x,y)\}$$

with

$$\gamma = \frac{\left(1 + \sqrt{1 + \frac{4\alpha}{\sigma_1^2}}\right)\left(1 + \sqrt{1 + \frac{4\alpha}{\sigma_2^2}}\right)}{\left(\sqrt{1 + \frac{4\alpha}{\sigma_1^2}} - 1\right)\left(\sqrt{1 + \frac{4\alpha}{\sigma_2^2}} - 1\right)}\,.$$

Both theoretically stated qualitative properties, supersolution and coincidence subset, have been verified by the numerical tests.

Table 4 summarizes the numerical results for five refinement levels from a uniform initial mesh with 289 nodes and 512 triangular elements. Moreover, the same stopping test in the relative quadratic error between two iterations and the same parameter β as in Example 1 have been chosen. As the exact solution cannot be computed, errors cannot be reported. We can observe that the ALAS algorithm exhibits much shorter computational time (t) and less iterations (I).

	ALAS				Projected Gauss–Seidel			
L	NE	NN	t_A	I_A	NE	NN	t_{GS}	I_{GS}
1	512	289	5.21	3	512	289	68.38	86
2	732	401	8.63	4	732	401	130.13	86
3	1275	675	19.41	6	1288	682	463.04	108
4	2367	1224	52.41	9	2445	1263	2743.57	190
5	4466	2277	133.67	11	4766	2428	14419.40	271

Table 4 Mesh refinement, computational time, iterations and errors obtained for Example 2. L, NE, NN, t and I represent the level of refinement, number of elements, number of nodes, computational time in seconds and number of iterations, respectively. When appearing, subindex A refers to ALAS algorithm and GS refers to projected Gauss-Seidel

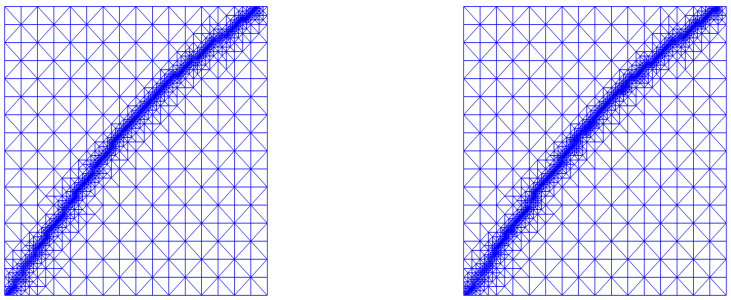

Fig. 2 Adaptive meshes of the domain $\mathcal{F}(\Omega)$ for ALAS (left) and projected Gauss-Seidel (right), after 5 refinement steps for Example 2

Figure 2 shows the meshes after five refinement levels. As in Example 1 the one corresponding to ALAS seems to follow a bit better the free-boundary (optimal investment boundary) of the problem. Notice that the region above and at the left of the free boundary corresponds to the part of the domain where $v = h$, while the region located below and at the right of the free boundary corresponds to $v > h$. Thus, for each value of the benefit (per unit) of the environment there exists a different critical value of the benefit (per unit) of the industrial project above which the optimal utility is equal to the one obtained if we start the investment at the initial time.

The associated numerical solutions at this refinement level with both numerical methods are shown in Figure 3 and are very close each other. The plane in black behind the solution represents the obstacle function h.

Example 3:

In this last example of the instantaneous irreversible case, the function h is given by (14), so that for the choice $f(x) = x$ the function G is

$$G(x, y) = x - \frac{(\alpha - \mu_2)y}{(\lambda - 1)(\sigma_2^2\lambda + \mu_2)},$$

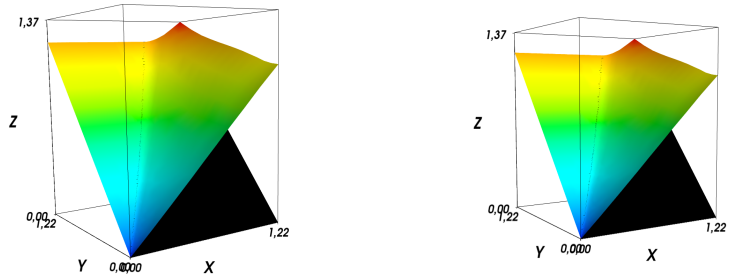

Fig. 3 Numerical solution for ALAS (left) and projected Gauss-Seidel (right), after 5 refinement steps for Example 2

with λ being given by (15). The financial parameters are shown in Table 5 so that an optimal investment boundary appears.

σ_1	σ_2	μ_1	μ_2	ρ	α
0.18	0.40	0.08	0.15	0.20	0.25

Table 5 Financial data set for Example 3

	ALAS				Projected Gauss–Seidel			
L	NE	NN	t_A	I_A	NE	NN	t_{GS}	I_{GS}
1	512	289	5.19	3	512	289	114.93	150
2	745	409	8.75	6	745	409	327.24	214
3	1296	688	19.66	9	1299	689	1506.50	350
4	2379	1231	52.97	12	2488	1287	7582.44	511
5	4583	2321	139.81	15	4686	2390	36982.91	725

Table 6 Mesh refinement, computational time, iterations and errors obtained for Example 3. L, NE, NN, t and I represent the level of refinement, number of elements, number of nodes, computational time en seconds and number of iterations, respectively. When appearing, subindex A refers to ALAS algorithm and GS refers to projected Gauss-Seidel

Table 6 summarizes the numerical results for five refinement levels from a uniform initial mesh with 289 nodes and 512 triangular elements. Moreover, the same stopping test in the relative quadratic error between two iterations and the same parameter β as in Example 1 are chosen. Again the ALAS algorithm exhibits much shorter computational time (t) and less iterations (I).

Figure 4 shows the meshes after five refinement levels. As in previous examples the one corresponding to ALAS seems to better follow the free-boundary of the problem. The associated numerical solutions at this refinement level are shown in Figure

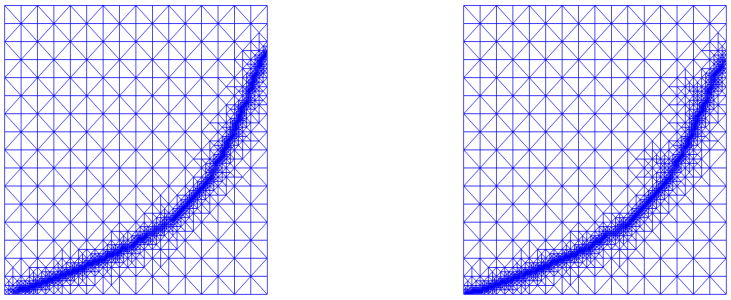

Fig. 4 Adaptive meshes of the domain $\mathcal{F}(\Omega)$ for ALAS (left) and projected Gauss-Seidel (right), after 5 refinement steps for Example 3

5. As in the previous examples, the mesh corresponds to the bounded domain ($\mathcal{F}(\Omega)$), while the solution is presented, jointly with the obstacle, over a bounded subdomain of the unbounded original domain Ω. In this case, the only theoretically stated qualitative properties are the bounds indicated in $[11, 1]$, which have been verified by the computed numerical solutions.

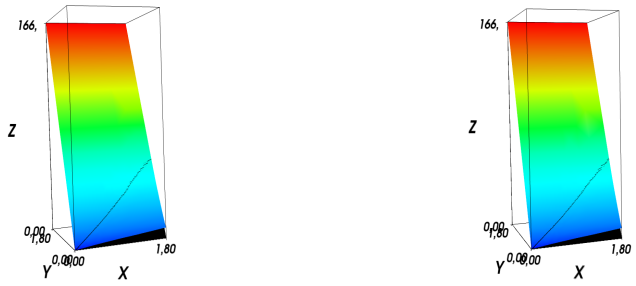

Fig. 5 Numerical solution for ALAS (left) and projected Gauss-Seidel (right), after 5 refinement steps for Example 3

4.2 Examples with progressive transformation

In this section we consider several examples in which the effect on the environment is not instantaneous. Following [21], we consider the additive HARA utility functions U given by expression (5) for different values of the p, where $1-p$ represents constant relative risk aversion parameter.

We consider the same parameters as in Example 2 in the instantaneous case (see Table 3). In this setting, we first consider the case $p = 1$, which corresponds to risk-

neutrality and a linear utility function. For this case, Figure 6 shows the computed numerical solution v for the values $\theta = 0.25$ and 0.75, associated to different initial transformed fractions of the environment. For each value of θ the corresponding regions $v_\theta = 0$ (blue) and $v_\theta < 0$ (red) are shown in Figure 7, with the free boundary separating both regions. Actually, we obtain these regions by considering $t = 1 - \theta$ and representing the regions where $u(\cdot, t) = \psi(\cdot, t)$ (blue) and $u(\cdot, t) > \psi(\cdot, t)$ (red).

The results have been obtained for a discretization time step $\Delta t = 0.025$ and a uniform mesh with $4,225$ nodes and $8,192$ triangular element. The parameters for the ALAS algorithm are the same as in the case of instantaneous effects.

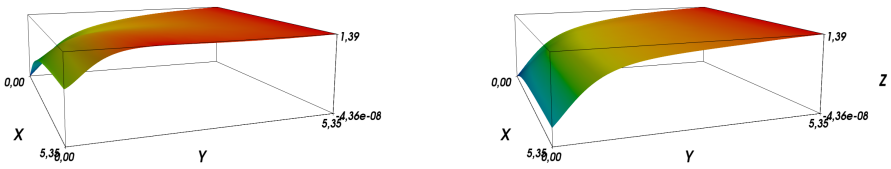

Fig. 6 Numerical solution for $\theta = 0.25$ (left) and $\theta = 0.75$ (right) with $p = 1$ in the progressive transformation case

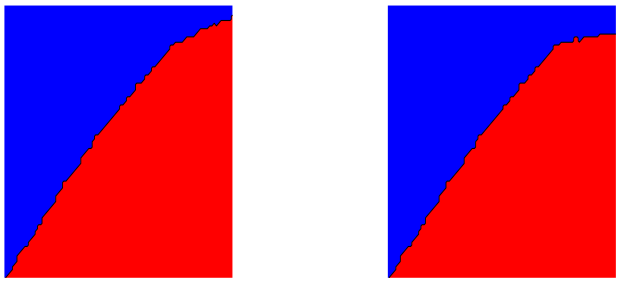

Fig. 7 Free boundary for $\theta = 0.25$ (left) and $\theta = 0.75$ (right) with $p = 1$ in the progressive transformation case

Next, Figures 8 and 9 show the analogous computed results for the case $p = 0.3$, thus corresponding to a nonlinear HARA utility function and the presence of risk aversion.

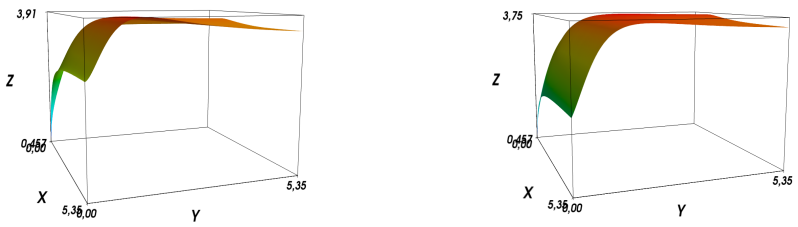

Fig. 8 Numerical solution for $\theta = 0.25$ (left) and $\theta = 0.75$ (right) with $p = 0.3$ in the progressive transformation case

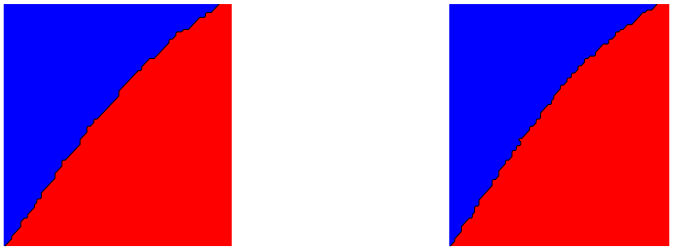

Fig. 9 Free boundary for $\theta = 0.25$ (left) and $\theta = 0.75$ (right) with $p = 0.3$ in the progressive transformation case

On the other hand, as indicated in [21], the homogeneity of degree p of U implies the same homogeneity for the value function v. Thus, for utilities given by (5) this homogeneity allows to reduce the dimension of the problem and analyze some qualitative properties of the function

$$w(y, \theta) = v(1, y, \theta) \tag{38}$$

We have used some of them to validate the here proposed numerical techniques. In particular, the free boundary that separates the region where where $w_\theta < 0$ from the region where $w_\theta = 0$ can be parameterized by a curve $y = g(\theta)$. The first region is characterized by $y \leq g(\theta)$ and no action should be taken in the associated singular control problem, while the second region corresponds to $y > g(\theta)$ and the optimal policy is to jump to the θ_0 such that $y = g(\theta_0)$. Moreover, the authors prove that

$$w(y, \theta) = w(y, 1), \qquad y \in [g(1), +\infty), \tag{39}$$

for all $\theta \in (0, 1)$. This means that for all values of θ the functions $w(., \theta)$ meat at the point $y = g(1)$ and take the same value after this point, as it is clearly illustrated in Figure 10 for $p = 1$. Moreover, the observed results are in agreement with the estimated value of $g(1) = 1.4945$ in [21]. In the region where $y > g(1)$ the optimal

policy leads to full conversion of the environment. On the other hand, when $y < g(0)$ the alternative project should not start until their benefits do not exceed those ones of the environment by a certain amount. For the risk-neutrality case ($p = 1$) the identity $g(0) = g(1)$ holds.

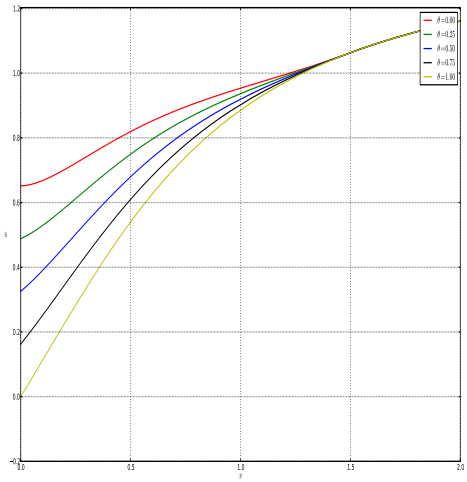

Fig. 10 Solution $w(\cdot, \theta) = v(1, \cdot, \theta)$ for different θ with $p = 1$ in the progressive transformation case

5 Conclusions

In this paper we address the numerical solution of investment problems with instantaneous and progressive irreversible effects on the environment. In the instantaneous case an obstacle problem associated to a degenerated elliptic equation is numerically solved. As illustrated by the numerical tests, more efficient methods than in the previous work of the authors [1] are proposed. More precisely, the computational time of the ALAS algorithm is much shorter than the projected Gauss Seidel. In the progressive case, following the formulation proposed in [8] the problem is formulated in terms of the subsequent solution of parameter dependent elliptic boundary value problems and an evolutive obstacle problem. After the time discretization, at each time step an obstacle problem associated to an degenerate elliptic equation is posed and solved with the same numerical techniques than in the instantaneous case. Numerical examples are partially validated with the qualitative properties obtained in [21] for the case of additive HARA utility functions. These properties are mainly based on a certain homogeneity property. Notice that the proposed numerical techniques can be applied to more general cases. However, the limit case $p \to 0$ corre-

sponding to unbounded utility at the origin will require further treatment from the theoretical and numerical point of view.

References

1. A. Acción, I. Arregui, C. Vázquez, *Numerical solution of a free boundary problem associated to investments with instantaneous irreversible effects*, Appl. Math. Comput., 215 (2010), 3461–3472.
2. K.J. Arrow, A.C. Fisher, *Environmental preservation, uncertainty and irreversibility*, Quaterly J. Econ., 88 (1974), 312–319.
3. A. Bensoussan, J. L. Lions, *Application des Inégalités Variationnelles en Control Stochastique*, Dunod, Paris, 1978.
4. A. Bermúdez, M. R. Nogueiras, C. Vázquez, *Numerical solution of variational inequalities for pricing Asian options by higher order Lagrange-Galerkin methods*, Appl. Numer. Math., 56 (2006), 1256–1270.
5. A. Brandt, C. W. Cryer, *Multigrid algorithms for the solution of linear complementarity problems arising from free boundary problems*, SIAM J. Sci. Stat. Comput., 4 (1983), 655–684.
6. M. C. Calvo-Garrido, A. Pascucci, C. Vázquez, *Mathematical analysis and numerical methods for pricing pension plans allowing early retirement*, SIAM J. Appl. Math., 73 (2013), 5, 1747–1767.
7. M.G. Crandall, H. Ishii, P.L. Lions, *User's guide to viscosity solutions of second order partial differential equation*, Bull. Amer. Math. Soc., 27 (1992), 1–42.
8. G. Díaz, J. I. Díaz, C. Faghloumi, *On an evolution problem associated to modelling of incertitude into the environment*, Nonlinear Analysis: Real World Applications, 8 (2007), 399–404.
9. J. I. Díaz, C. Faghloumi, *Analysis of a degenerate obstacle problem on an unbounded set arising in the environment*, Appl. Math. Optim., 45 (2002), 251–267.
10. A. K. Dixit, R. S. Pindyck, *Investment under Uncertainty*, Princeton University Press, Princeton, NJ, 1994.
11. C. Faghloumi, *Modelización y tratamiento matemático de algunos problemas en medio ambiente*, Ph. D. Dissertation, Universidad Complutense de Madrid, 2003.
12. A.C. Fowler, *Mathematical Geoscience*, Springer, 2011.
13. R. Glowinski, J. L. Lions, R. Tremolières, *Analyse Numérique des Inéquations Variationnelles*, Dunod, Paris, 1976.
14. R. H. W. Hoppe, *Multigrid methods for variational inequalities*, SIAM J. Numer. Anal., 24 (1987), 1046–1065.
15. R. Kangro, R. Nicolaides, *Far field boundary conditions for Black–Scholes equations*, SIAM J. Numer. Anal., 38 (2000), 1357–1368.
16. T. Kärkkäinen, K. Kunisch, P. Tarvainen, *Augmented Lagrangian active set methods for obstacle problems*, JOTA, 119 (2003), 499–533.
17. D. Kinderlehrer, G. Stampacchia, *An Introduction to Variational Inequalities and their Applications*, Academic Press, New York, 1980.
18. R. Kornhüber, *Monotone multigrid methods for elliptic variational inequalities I*, Numer. Math., 69 (1994), 167–184.
19. J. L. Lions, B. Mercier, *Approximation numérique des équations de Hamilton–Jacobi–Bellman*, RAIRO Anal. Numér., 14 (1980), 369–393.
20. M. C. Rivara, *Algorithms for refining triangular grids suitable for adaptive and multigrid techniques*, Int. J. Numer. Meth. Engrg., 20 (1984), 745–756.
21. J. A. Scheinkman, Th. Zariphopoulou, *Optimal environment management in the presence of irreversibilities*, J. Econom. Theory 96 (2001), 180–207.